Determination of the Shear Strength Parameters of Flow Band Structures in Andesites under Static and Dynamic Conditions

Ahmet Turan ARSLAN*, Bayram KAHRAMAN

Dokuz Eylül University, İzmir Vocational School, Buca, İzmir/TURKEY
(ORCID: 0000-0002-8018-1707)
Department of Mining Engineering, Engineering Faculty, Dokuz Eylül University, Buca
İzmir/TURKEY (ORCID: 0000-0001-9429-6591)

Abstract: Stability and deformation analyses of geotechnical projects such as tunnels, underground excavations and rock slopes require reliable data about the behavior of discontinuities (joints, fractures, bedding planes and etc.). Therefore, shear box tests are widely used in rock mechanics applications. In this study, several static and dynamic shear box tests were carried out both over flow bands of the andesites which cover a large area in the northern part of Izmir Bay. Shear box tests were conducted under both static and dynamic conditions on rectangular planes with a dimension of 400 x 200 mm. As a result of these tests, normal displacement-normal stress, shearing displacement-shearing stress and normal displacement-shear strength correlations were obtained. Also, peak and residual shear strength values, base friction angle and residual friction angle were found and the results were interpreted. Thus, the shear strength properties of the flow band structures can be given with more accuracy. Based on the new findings, more realistic solutions will be obtained in numerical analyses and simulation models aiming at determining the stability of underground excavations and engineering projects on the ground surface will be more reliable.

Andezitlerdeki Akma Bantlarının Makaslama Dayanım Parametrelerinin Statik ve Dinamik Koşullar Altında Belirlenmesi

Özet: Tüneller, yeraltı kazıları kaya şevleri gibi jeoteknik projelere ait stabilite ve deformasyon analizleri, süreksizliklerin (eklemler, çatlaklar, tabakalanma düzlemleri vb.) davranışları hakkında güvenilir verilere ihtiyaç duymaktadır. Bu nedenle makaslama kutusu deneyleri, kaya mekaniği uygulamalarında yaygın bir şekilde kullanılmaktadır. Bu çalışmada, İzmir Körfezi kuzeyinde geniş alanlar kaplayan andezitlerdeki akma bantları üzerinde statik ve dinamik koşullarda makaslama kutusu deneyleri

yapılmıştır. Makaslama deneyleri 400 x 200 mm dikdörtgen şekilli geniş yüzeyler üzerinde statik ve dinamik koşullarda yapılmıştır. Statik koşullarda yapılan deneylerde, zaman – yer değiştirme; zaman – gerilme; makaslama yer değiştirmesi – gerilme; makaslama yer değiştirmesi – normal yer değiştirme; makaslama yer değiştirmesi – makaslama gerilmesi; normal gerilme – makaslama gerilmesi ilişkileri elde edilerek doruk ve artık makaslama dayanımları, temel sürtünme açısı ve artık sürtünme açısı değerleri bulunarak sonuçlar yorumlanmıştır. Dinamik koşullarda yapılan deneylerde ise, makaslama yer değiştirmesi – zaman, makaslama gerilmesi – zaman, makaslama yer değiştirmesi – makaslama gerilmesi – zaman, makaslama gerilmesi – makaslama yer değiştirmesi, normal yer değiştirme – zaman ilişkileri elde edilmiş ve sonuçlar yorumlanmıştır. Andezitlerdeki akma bantlarında yapılan makaslama kutusu deneyleri sonucunda; akma bantlarının dayanım özellikleri daha gerçekçi olarak tanımlanacak, nümerik analiz programları ve nümerik simülasyonlar kullanılarak depremlere bağlı olarak andezitlerdeki yer altı ve yerüstü kaya yapılarının duraylılığını belirlemeye yönelik modellemelerde daha gerçekçi çözümler elde edilecektir

*Sorumlu yazar: ahmet.arslan@deu.edu.tr

1. Introduction

Most of the rock mass has discontinuities such as bedding planes, joints, shear zones and faults. Failures are rarely seen in rock material in the shallow depths having low stress and the behaviour of the rock mass is controlled by discontinuities. To analyze a rock block's stability, factors controlling shear strength of the discontinuities separating rock blocks must be considered. Rock mass properties should be revealed after field works and design must be conducted using the data. Izmir is considered one of the most irregular urbanized cities in Turkey. Especially, this problem is faced with in the southern and northern districts of the Izmir Bay Koca (1995), Koca and Kıncal (2004). Discontinuity controlled instabilities are frequently seen in andesites in the region. Falling, toppling and sliding type slope movements are observed around existing slope cuts and abandoned stone quarries. Rock units provide a suitable base for foundations unless they are highly fractured, weathered and porous media. Geotechnical properties of rocks include discontinuities, thickness of the rock unit, weathering grade and porosity. Safe bearing capacity of rock mass will be decreased if it is highly fractured. Even if they bear the overlying loads safely, there will be shear deformations because of the opening and sliding of the discontinuities. For this reason, positions (attitudes) and properties of the discontinuities which foundations will be placed on is critical. Resistance parameters (e.g. c, ϕ) which affect the shear stresses must be determined precisely to judge the problem mentioned above. These parameters are determined via portable (in-situ) or in laboratory-designed shearing testing devices (Jing et al., 1993; Geertsma, 2002; Seidel and Haberfield, 2002; Kim et al., 2006; Wang el al., 2007; Gomez et

al., 2008; Buzzi et al., 2008; Barla et al., 2007, 2010; Konietzky et al., 2012b). The shear behaviour of rock joints has been investigated by many researchers under both constant normal load (Barton, 1976; Gentier, et al., 2000; Grasselli and Egger, 2003; Belem, et al., 2004; Jiang, et al., 2006; Kim and Lee, 2007; Asadi and Rasouli, 2012) and constant normal stiffness (Ohnishi and Dharmaratne, 1990; Kodikara and Johnston, 1994; Haberfield and Seidel, 1999; Haque, 1999; Jiang, et al., 2004).

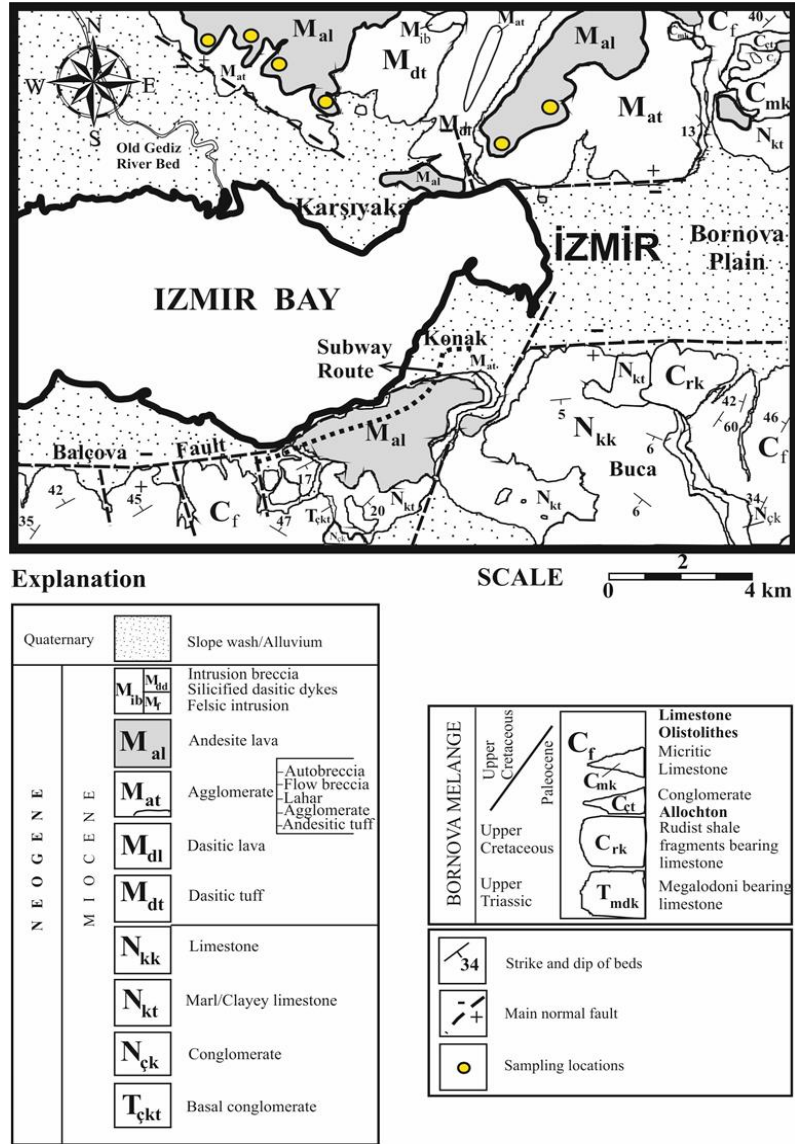## 2. Geology of the Study Area

The Upper Cretaceous-Paleocene aged Bornova Melange rocks exposed in Izmir Metropolitan area mainly consist of conglomerate, micritic limestone, Bornova Flysch and limestone olistolithes in the flysch matrix. Bornova Melange is highly folded and fractured by the effect of tectonic activities. Neogene sedimentary rocks, consisting of conglomerate, sandstone, siltstone, mudstone, and limestone, discordantly overlie the melange (Fig.1) Miocene volcanics mainly consisted of dasitic tuff, dasitic lava, and andesitic lava subunits, were identified and mapped. Modern faults and shear zones are developed from the cooling joints in the andesitic and dasitic lavas. Shear zones which are parallel to the cooling joints strike in NE-SW direction, are especially wide spread in south of the bay (Koca, 1995). The similar shear zones in north of the bay can be seen in abandoned stone quarries. The major cooling joints in the andesitic and dacitic lavas strike NE-SW and NW-SE directions were affected by the tectonic activities.

surfaces can be smooth or rough; in good contact or poor contact; filled or not. Rock mass behaviour under low stress conditions is mostly controlled by sliding along existing discontinuities rather than failure of the intact rock mass (Hoek, 2007). This means that the shear strength of a discontinuity in rock mass may have a strong impact on the mechanical behaviour of rock joints in engineering structures (slopes, foundations, tunnels, etc.). The behaviour of rock discontinuities is still not very well investigated and understood in general and especially under dynamic loads. Large-size underground structures such as storage caverns and radioactive waste repositories or dams require a high standard of resistance against blasting and earthquake loads. Therefore, the dynamic shear behaviour of rock joints becomes more important for engineers (Nguyen, 2013). The most popular method currently used to determine the joint shear strength is a direct shear test which can be performed in the field and in the laboratory using a direct shear apparatus. The shear behaviour of flow bands is studied in laboratory under CNL (Constant Normal Load) and dynamic boundary conditions.

Rock masses comprise rock material as well as discontinuities and the effects of the discontinuities on rock mass must be determined for engineering applications. Therefore, scan-line works have been done to determine the properties of flow band structures by Koca and Kıncal (2004) and Koca et al. (2006) according to ISRM (1981).

3. Shear Strength of Andesitic Flow Bands

Natural rock masses always contain discontinuities. The discontinuity

Figure 1. Simplified geological map of the Izmir metropolitan area and locations of the andesite quarries (Koca, 1995)

Attitudes of the flow band structures obtained with the help of scan-line works and detailed properties of the flow bands were given in Table 1

Table 1. Flow bands properties obtained from scanlines (Koca and Kıncal 2004)

Flow bands	
Bedding plane and joint spacing	1-3 cm (moderately narrow) generally closely spaced joints
Width of apertures	Generally closed joints
Persistence	1.5– 3.5 m low persistence

Table 2. The values of the first and second order asperity angles measured on the profiles for the flow band surfaces

Location	Discontinuity type	The number of measurements		Mean second order asperity angle (degree) (i_2)	Mean first order asperity angle (degree) (i_1)
		For the first order asperity	For the second order asperity		
Osmangazi quarries	Flow bands	38	338	20.97±9.55	14.40±3.28

In-situ and laboratory roughness measurements were carried out on flow band structures in andesites and presented in Table 2. And also, a graph was prepared to show the second order asperities is also given in Fig. 2. It can be said that flow band surfaces are rough, very rough and undulating according to the classification suggested by ISRM (2007). A contour diagram was prepared for the Osmangazi Quarry-4 using 84 field measurements (Fig.3). Pole concentration point is obtained from the contour diagram (Fig.3). To carry out shear box tests on flow band surfaces, six block samples were obtained in the locations where scan-line works were conducted. The range of normal stress was chosen as 3-10-15-20 MPa to represent the field conditions and used during the tests. During the shear box tests, GS 1000 shear box test equipment were used in TU Bergakademie Freiberg İnstitüt für Geotechnik Gesteinsmechaniklabor, Germany. GS 1000 shear box device has the maximum capacity of 1000 kN normal force, 300 kN tensile force, + 800 kN shear force, ± 500 kN dynamic load (40 Hz) for both directions.

4. Mechanical, Elastical and Dynamic Properties of Andesites

Andesite block samples were obtained in northern part of the Izmir Bay to determine mechanical, elastical and dynamic properties of andesites, behavior models during earthquakes experimentally, empirically and with the help of mathematical models and to determine what kind of movement foundations on andesites will be exposed to. Core samples obtained from the rock block samples and physical and mechanical properties of the andesite core samples were tested in TU Bergakademie in Germany. Compression wave velocity (V_P), Shear wave velocity (V_S), Dynamic Elasticity Modulus (E_D), Shear Modulus (G), Poisson's Ratio (ν) parameters were determined for andesite samples using the Ultraschall-generator USG21 Geotron-Elektronik Transienten-Recorder TRB 4000 seismic analyzer according to ISRM (2007) and results were given in Table 3.

Uniaxial compressive strength (UCS) tests (loading-unloading stepped) were conducted using TIRAtest 28500 test device applying 2.0 MPa/min on a rock unit according to DGGT (2004b) and results were given in Table 4. Static triaxial compressive strength (STCS) tests were conducted using MTS 815 test device applying axial force at a rate of 4 kN/min and confining pressure at 1 MPa/min on three rock units according to ISRM (1983). Results are given in Table 5. Dynamic triaxial compressive strength (DTCS) tests were conducted using MTS 815 test device. After applying a static axial force at a rate of 4 kN/min and confining pressure at 1 MPa/min dynamic (cyclic) axial loading was superimpozed with a dynamic

peak-to-peak-amplitude of 5 kN at a frequency of 2.0 Hz for 300 s. After a dynamic loading sequence the center amplitude was raised 8 (n_{dyn}) times by the step value of 2.55 MPa ($\Delta\sigma_{dyn}$). Loading parameters are given in Table 6.

5. Shear Testing Device

The most commonly used method for testing the shear behaviour of rock joints is the direct shear test. This type of test is usually carried out in the laboratory, but it may also be performed in the field. In recent years, several commercial

producers have developed shear box devices for rock mechanical testing (e.g. MTS-816, GCTSRDS-500, TerraTek-DS-4250, LO-5010, HR72.340).

The technical data show maximum normal forces between 500 kN and 1500 kN, maximum shear forces between 250 kN and 750 kN and maximum shear box dimensions between 100 mm and 350 mm. A summary of technical data for several direct shear box devices is presented in Table 7.
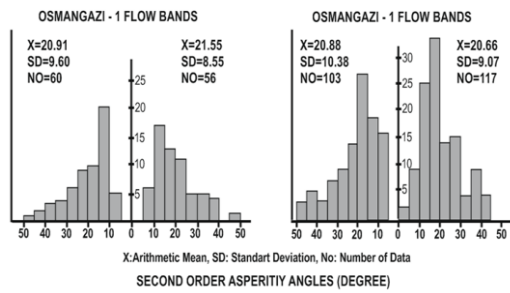
Figure. 2 Frequency distributions of the second order asperity angles of flow bands.
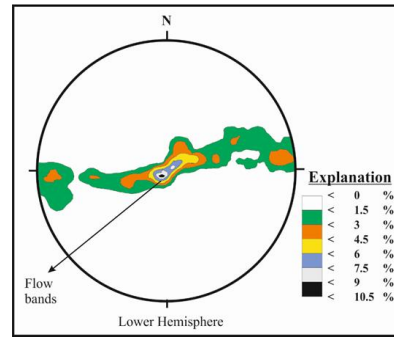
Figure 3. Contour diagram prepared using the flow band orientations of andesites from the northern part of Izmir Bay.

Table 3. Dynamic elastic coefficients of the samples.

Lithological Unit	V_P Wave Velocity (m/sn)	V_S Wave Velocity (m/sn)	Elastisity Modulus (GPa)	Shear Modulus (GPa)	Poisson's Ratio
	4138	2544	35.66	14.91	0.20
Andesite	4245	2608	38.44	16.06	0.20
	4126	2437	33.43	13.57	0.23

Table 4. Loading-unloading stepped uniaxial compressive strength test results.

Lithological Unit	UCS (σ_c) (MPa)	Modulus of Deformation (GPa)	Young's Modulus (GPa)	
			Unloading Cycle	Reloading Cycle
Andesite	72.11	23.68	34.76	35.18

UCS (σ_c): Uniaxial Compressive Strength

Table 5. Triaxial compression test results. Stresses at peak strength are given.

Lithology	(σ_3) (MPa)	(σ_1) (MPa)	$(\sigma_1 - \sigma_3)$ (MPa)	Internal Friction Angle (ϕ) (°)	Cohesion (c) (MPa)	Elasticity Modulus (GPa)	Poisson's Ratio (ν)
	5.0	38.40	33.40			16.55	-
Andesite	10.0	74.14	64.14	35.20	8.00	20.48	-
	20.0	92.02	72.02			27.83	0.36

Table 6. Dynamic triaxial compression test results

Lithology	(σ_3) (MPa)	$(\sigma_{1stat.\ max})$ (MPa)	$(\sigma_{1dyn\ min})$ (MPa)	$(\sigma_{1dyn\ max})$ (MPa)	$(\Delta\sigma_{dyn})$ (MPa)	f_{dyn} (Hz)	t_{dyn} (sn)	n_{dyn}
	5.00	-	-	-	-	-	-	-
Andesite	10.00	49.4	-	-	-	-	-	-
	20.00	-	65.0	85.4	2.55	2.00	300	8

Table 7. Main technical data of some direct shear box devices

Direct shear apparatus	Technical Data				
	Normal Force (kN)	Shear Force (kN)	Max. shear displacement (mm)	Shear box dimensions (mm)	Dynamic testing
MTS-816	500	250	100	200 x 200 x 340	No
GCTS-RDS-500	1500	300	50	100 x 100 x 150	No
TerraTek-DS-4250	1000	300	50	150 x 150 x 300	No
HR72.340	500	750	-	350 x 350 x 450	No
LO-50100	500	500	50	150 x 250	Yes
Huang (1993)	500	500	7	200 x 150	Yes
Barbero (1996)	9.51	17.2	20	100 x 100	0 ÷3.5 Hz
Kana (1996)	333.6	222.4	-	203 x 203 x 101	Yes
Boulon (1995)	100	100	-	100 x 100	No
Gehle (2002)	150	150	20	250 x 50 x 150	No
Hans (2003)	100	100	-	100 x 100	Yes
Jiang (2004)	400	400	-	500 x 100	No
Kim (2006)	150	150	25	140 x 75	No
Gomez (2008)	200	200	305	711 x 406	No
Barla (2010)	100	100	18	ϕ100	No
Konietzky (2012)	1000	800	50	400 x 200 x 160	0÷40 Hz

Beside that, several researchers (Geertsma 2÷02, Gehle 2002, Seidel & Haberfield 2002, Jiang et al. 2004, Kim et al. 2006, Gomez et al. 2008, Barla et al. 2010, Konietzky et al. 2012a, Konietzky et al. 2012b, Nguyen 2013) have designed and constructed their own shear box devices to perform direct shear tests. Dynamic shear box testing was reported by several researchers [*Huang, et al.*, 1993; *Ahola, et al.*, 1996; *Bakthar and Barton* 1984; *Barbero, et al.*, 1996; *Kana, et al.*, 1996; *Fox, et al.*, 1998; *Homand-Etienne, et al.*, 1999; *Lee, et al.*, 2001; *Jafari, et al.*, 2003; *Wang, et al.*, 2007; *Buzzi, et al.*, 2008]. However, these dynamic shear box devices were developed for tests on significant smaller samples and they are of quite different types. Barbero et al. (1996) have designed and constructed a direct shear testing machine with the purpose

of testing rock joints under both static and dynamic conditions. Loading capacity of this apparatus in dynamic condition is 10 kN, and the frequency range covers 0.01 ÷ 3.5 Hz. Kana et al. (1996), Ahola et al. (1996) and Fox et al. (1998) developed direct shear testing devices with higher load capacity up to 222 kN and frequencies up to 1.4 Hz. Lee et al. (2001) have designed a servo-controlled direct shear testing machine and attached it to a MTS 815 loading frame. The loading capacity of the testing system is 250 kN and allows cyclic shear motion of up to ± 60 mm displacement. Jafari et al. (2003) used the shear apparatus BCR-3D developed by Boulon (1995) to investigate the effect of cyclic displacements on shear strength of rock joints. Barla et al. (2010) have designed and developed a new direct shear testing apparatus for either soil or soft rock. The maximum loading capacity in the axial and in the shear direction is 100 kN and the maximum shear displacement is 18 mm. Ferrero et al. (2010) developed a new apparatus based on MTS 810 to investigate the behaviour of a rock discontinuity under monotonic and cyclic loads (Nguyen, 2013). A new direct shear device (GS 1000) was developed and installed at the rock mechanics laboratory at the Geotechnical Institute of the TU Bergakademie Freiberg to perform direct shear tests under static, dynamic and hydro-mechanical coupled conditions with extreme high loads (up to 1000 kN), big shear box dimensions (up to 400 x 200 mm^2) and dynamic loads up to 40 Hz with force amplitudes of up to ± 500 kN in both normal and shear directions (Fig. 4). The main technical data of the new direct shear box device GS-1000 are summarized in Table 8.
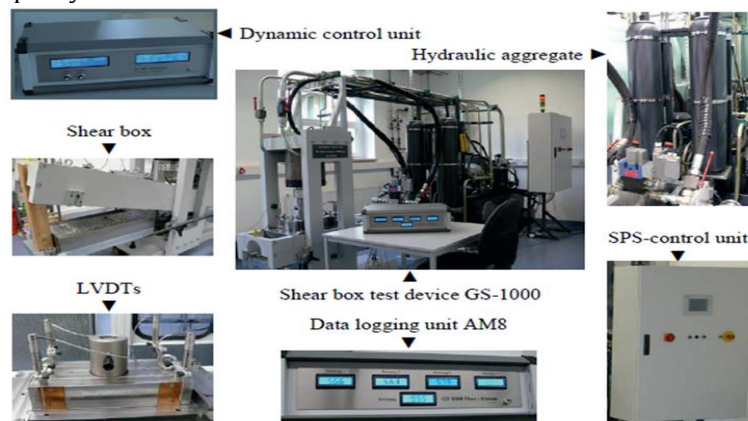
Figure 4. Overview of direct shear test apparatus GS1000

Table 8. Technical data of the GS-1000 apparatus

Parameter	Unit	Value
Maximum shear displacement	mm	50
Shear force	kN	-300 ÷ +800
Normal force	kN	0 ÷ 1000
Shear box size (LxWxH)	mm	200 x 400 x 160
Frequency	Hz	0 ÷ 40 (>40)
Dynamic loading	kN	± 500
Water pressure (hydro-mechanical coupling)	MPa	10

5.1. Direct Shear Box Testing Methods

There are two main methods usually used in the laboratory to investigate the shear behaviour of rock joints. They are called constant normal load (CNL) and constant normal stiffness (CNS) tests. CNL means that the normal lo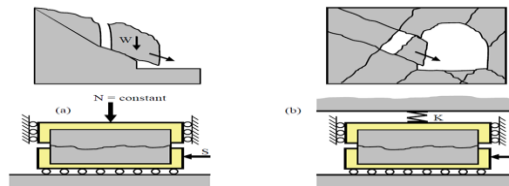ad is maintained constant during the shearing process. Shear testing under CNL boundary condition is suitable for cases such as non-reinforced rock slopes, where the surrounding rock mass freely allows the joint to shear without restricting the dilation, therefore, the normal load on the shear plane is constant during shear process as shown in Figure 5a.
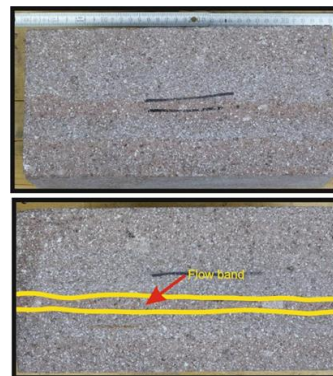

Figure 5. Overview of direct shear test apparatus GS1000

CNS means that the normal stiffness is maintained constant during the shearing process (Figure 5b). Shear testing under CNS boundary condition is usually suitable to investigate the behaviour in deep underground openings or in rock bolt reinforced slopes, where the surrounding rock mass is unable to deform sufficiently and the normal stress acting on the shear plane is not kept constant during the shearing process. In this case, the dilation is controlled by the normal stiffness of the surrounding rock mass. Therefore, the normal stresses on the shear plane increase or decrease with increasing or decreasing dilation, respectively.

6. Laboratory Shear Box Tests

6.1. Shear Strength of Flow Bands Under Static Loading

Shear strength is the maximum resistance to deformation by continuous shear displacement upon the action of shear stress. 15x15x30 cm size, total of 6 block sample, locations given in Figure 1, were obtained to determine shear strength parameters of andesite flow bands under static conditions (Fig. 6; Fig. 7).

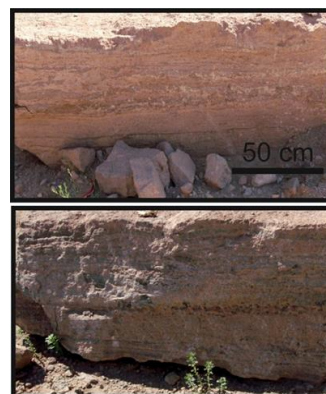**Figure 6**. Block sample prepared for shear box test.

Figure 7. A view of andesite block samples in the field

The sample preparation and the direct shear tests were conducted according to the recommendation of ISRM (1974) and ASTM (2002). The block samples were placed in the GS 1000 test apparatus and loaded with constant normal stress levels of 3 MPa, 10 MPa, 15 MPa and 20 MPa, respectively. During all tests shearing was applied parallel to the flow bands surfaces. Constant shearing displacement velocity was applied with the help of SPS S7 control unit while measurement values for shear and normal deformation were obtained directly at the specimen with AM8 measuring system (Fig.8).

The normal load is measured by a load-cell integrated into the vertical load piston. The shear load is measured by another load-cell connected to the horizontal load piston. Horizontal and vertical displacements are measured by LVDT's (Linear Variable Differential Transformer). Vertical displacement is measured at the four corners at the upper shear frame. Horizontal displacement is measured by a LVDT fixed to the lower shear box part as shown in Figure 8. Accuracy in displacement measurements is in the order of 1 μm.

During the shear box test shearing movement was started parallel to the flow band surface in the first stage and during the 760 seconds period, 10 mm shear displacement was applied from left to right under 3 MPa constant normal stress (CNL). Peak shear strength was reached to 5.90 MPa value in the first stage and decreased from this peak point to 2.50 MPa residual shear level. In the second stage, the point moved in such a manner that will be opposite direction (from right to left). In 1340 seconds, there was a shear displacement of 20 mm. during that period. At this step, residual shear strength increased from 2.50 MPa to 3.0 MPa. In the third and final step, the shear displacement moved again from the left to the right by 10 mm in 650 seconds back to the point at which the test started. In this last step the residual shear strength of the flow band structures was measured as 2.30 MPa (Fig. 9a, Fig. 9b; Fig. 10a, Fig. 10b). During the shear box test, sample showed elastic behavior with small displacements, force which resist shearing strength exceeded after the linear increase in shear strength and shear displacement, stress-displacement relation lost its linearity and peak shear strength of flow band reached a value of 11.20 MPa under 10 MPa constant vertical stress. From this point, shear stress decreased to 7.50 MPa residual shear strength (Fig. 11a; Fig. 11b).
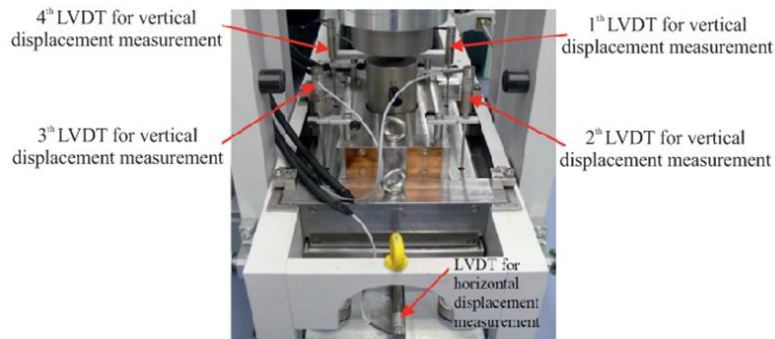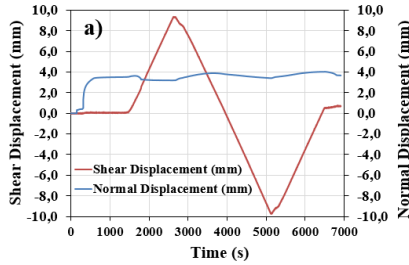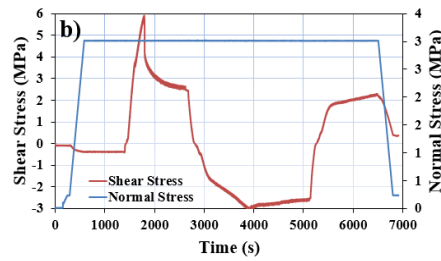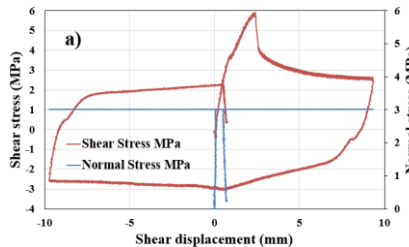

Figure 8. LVDT's view for the normal and shear displacement measurement.
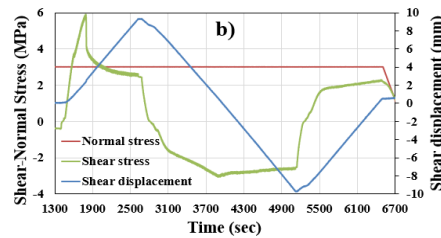
Figure 9a. Relationship between time - normal displacement and shear displacement under the 3 MPa normal stress.
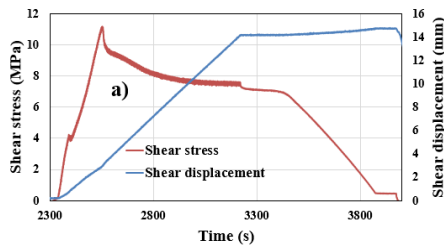

Figure 9b. Relationship between time - shear stress and normal stress under the 3 MPa normal stress.
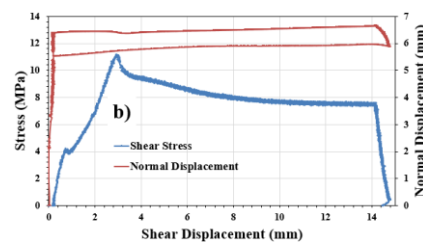

Figure 10 a. Relationship between normal stress, shear displacement and shear stress under the 3 MPa normal stress.

Figure 10 b. Shear test: stresses and shear displacement versus time.

Figure 11 a. Relationship between time-shear stress and shear displacement under the 10 MPa normal stress.

Figure 11 b. Relationship between shear stress, shear displacement and normal displacement under the 10 MPa normal stress.

Shear strength increased with the increase in the normal stresses on flow band structures and vertical displacement decreased and shear displacement became horizontal under the 15 MPa and 20 MPa vertical stress. There is no significant decrease observed in shear strength after the shear failure point under the 15 MPa and 20 MPa vertical stresses (Fig. 12a, Fig. 12b; Fig. 13a, Fig.13b). The behavior of the rock resembles ductile behavior in deformability test (σ-ε) (Fig.15).

Shearing surfaces in between upper shear frame and lower shear frame, formed after shear box tests under the constant normal load conditions, were photographed in detail and were given in Figure 14.
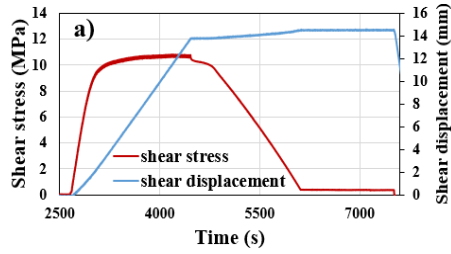
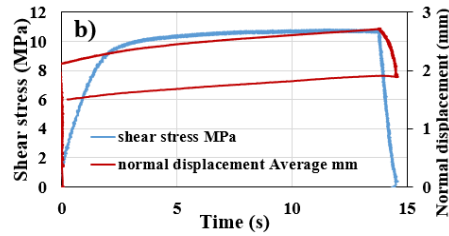**Figure 12a.**) Relationship between time, shear stress and shear displacement under the 15 MPa vertical stress.

Figure 12 b. Relationship between shear stress, shear displacement and normal stress under the 15 MPa vertical stress.
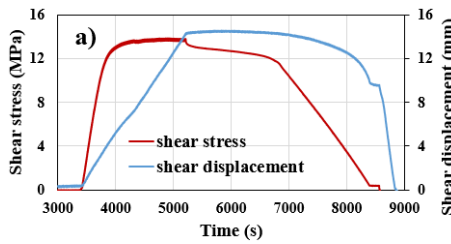

Figure 13 a. Relationship between time, shear stress and shear displacement under the 20 MPa vertical stress.
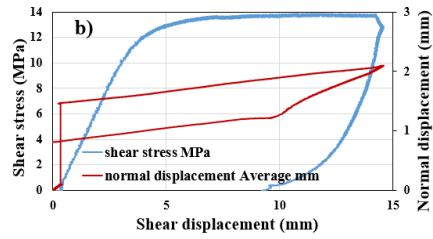
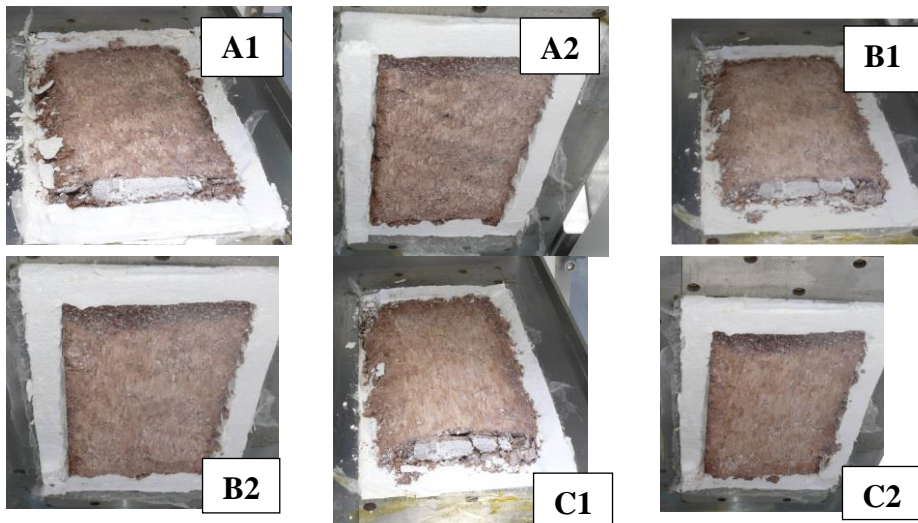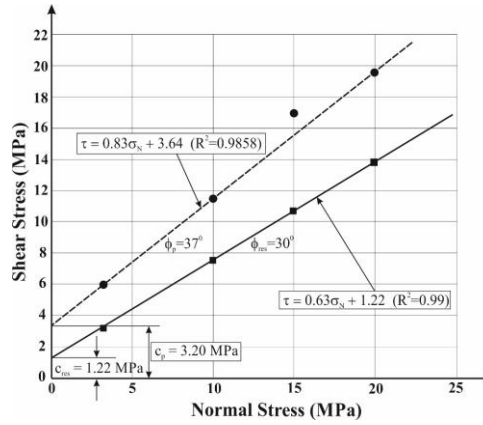**Figure 13 b.** Relationship between shear stress, shear displacement and normal stress under the 20 MPa vertical stress.

σ_N = 10 MPa A1: Sheared top surface, A2: Sheared bottom surface,
σ_N = 15 MPa B1: Sheared top surface, B2: Sheared bottom surface,
σ_N = 20 MPa C1: Sheared top surface, C2: Sheared bottom surface,

Figure 14. A view from sheared surfaces after the shear box tests.

Figure 15. Mohr-Coulomb failure envelope for peak and residual state for flow bands in andesite

6.2. Shear Strength of Intact Rock

Figure 15 shows that shear stress of intact rock increases linearly (elastic behaviour) with increasing shear displacement until peak shear strength is reached. After that the shear stress decreases until the residual shear strength (plastic behaviour) is reached. Peak and residual shear strength of intact rock increase as normal load increasies. Peak and residual shear stress of intact rock obtained from laboratory tests under various normal stresses are summarized in Table 9.

Table 9. Peak and residual shear stresses for initial intact rock samples

Sample	Normal stress σ_n (MPa)	Peak shear stress τ_P (MPa)	Residual shear stress τ_R (MPa)
1	3.0	6.0	3.0
2	10.0	11.7	7.5
3	15.0	17.2	10.7
4	20.0	19.7	13.8

Based on the peak and residual shear stresses of flow bands, the Mohr-Coulomb envelope is constructed for both peak and residual states as shown in Figure 15:

peak state:

$$\tau_P = 0.75\sigma_n + 3.64 \ (R^2: 0.9858) \qquad (1)$$

$c_P = 3.64$ MPa; $\phi_P = 37°$

residual state:

$$\tau_R = 0.58\sigma_n + 1.22 \ (R^2: 0.99) \qquad (2)$$

obtained as;

$c_R = 1.22$ MPa; $\phi_R = 30°$

Where;

τ_P is the peak shear strength,
τ_R is the residual shear strength,
σ_n is the normal stress,
ϕ_P is the peak internal friction angle,
ϕ_R is the residual internal friction angle,
c_P is the peak cohesion, and
c_R is the residual cohesion.

6.3. Shear Strength of Flow Bands Under Dynamic Loading

The dynamic effect in this work on jointed rock need to be considered. The shear behaviour of joints under dynamic conditions have been studied by many researchers (Bakhtar and Barton, 1984; Barla, et al., 1990; Hobbs, et al., 1990; Hutson and Dowding, 1990; Jing, et al., 1993; Qiu, et al., 1993; Kana, et al., 1996;

Divoux, et al., 1997; Belem, et al., 2007; Ferrero, et al., 2010; Konietzky, et al., 2012).

Behaviours of the discontinuities under repetitive loads are investigated according to their strain-deformation and strength properties. Strain-deformation properties involve dynamic bulk (shear) modulus and damping ratio values and their changes depending on unit deformations, and strength properties involve amplitude of shear stress and number of cycles which cause major deformations. Dynamic shear box tests are conducted to determine the behaviours of the discontinuities under repetitive loads. Field behaviour of the discontinuities can be estimated using empirical equations obtained from laboratory tests.

The block sample (15x15x30 cm) was placed in the GS 1000 test apparatus and fixed value of 3 MPa normal stress was applied during the test. Maximum displacement amplitude was applied as (u_{max}) ±10.0 mm under the 3 MPa normal stress. Shear displacement was allowed as 100 cyle in 110 seconds duration. Parameters for dynamic shear testing are given in Table 10. The shear displacement controlled sinusoidal excitation was applied horizontally to lower half of specimen as follows:
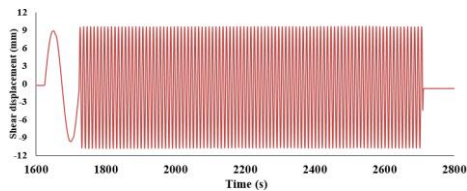
$$u_s = u_{max} \sin (2\pi ft) \tag{7}$$

where;
u_s is the shear displacement,
u_{max} is the maximum amplitude of shear displacement,
f is the frequency, t is the time.

Table 10. Parameters for dynamic shear testing

Parameters				
LxWxH (cm³)	σ_N (MPa)	f (Hz)	u_{max} (mm)	Num. of cycle
15x15x30	3.0	0.1	10.0	100

The shear displacement was measured by a horizontal LVDT which is attached to the bottom part of shear box. The normal displacement is also measured by four vertical LVDTs which are positioned at the four corners of the upper part of shear box. The measured shear displacement versus time (100 cycles) for the one tested specimen is illustrated in Figure 16.

The measured shear stress versus time for flow bands is shown in Figure 17. The measured peak shear stresses slightly increase with increasing time and number of cycles, respectively, as shown in Figures 17. This behaviour of the flow bands under dynamic loading is similar to the reported results by Homand-Etienne et al. (1999).
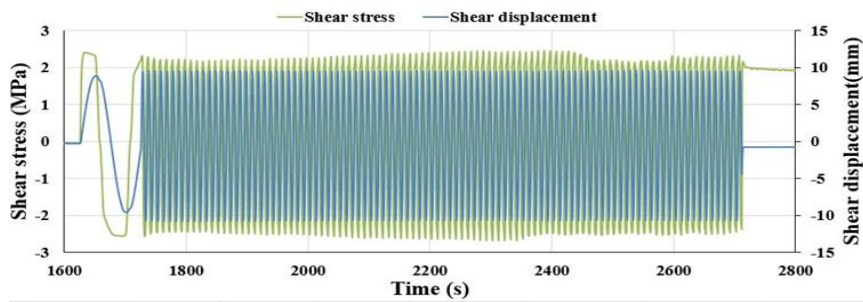

Figure 16. Shear displacement versus time of flow bands in andesitic Rock
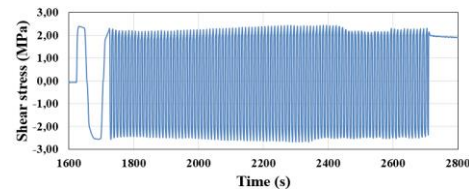
Figure 17. Shear stress versus time of flow bands in andesitic rock

Experimental results show that the absolute peak shear stress in the negative phases is higher than peak shear stress in the positive phases for flow bands in andesites rock. However, the peak shear stress in positive phases of the flow bands is slightly higher than absolute peak shear stress in the negative phases. The maximum shear stress in the positive and negative phases are given in Table 11.

Table 11. Absolute maximum shear stress

Absolute maximum shear stress (MPa)		Cycle number
Positive phase	2.43	71
Negative phase	2.70	58

Figure 18 shows the measured shear stress and shear displacement versus time for the dynamic test. This figure reveals a phase shift between shear displacement and shear stress. The shear displacement is phase lagging in comparison with the shear stress. This behaviour of flow bands under dynamic loading was observed during all experiment. These observed results are similar to the results reported by Ahola et al. (1996). The reason for the phase shift between shear stress and shear displacement is associated with chatter of the joint surface and vibrations of the apparatus as reported already by Ahola et al. (1996).

Figure 18. Shear stress and shear displacement versus time of flow bands

The most important issue in many problems of discontinuities under dynamic loads is the relationship between shear strength and unit strain. The relationship between shear strength and unit strain is obtained as a histerisis curve at the end of a full cyle of loading. Stress-strain behavior of the flow bands of andesites under the 100th loading cycle in dynamic shear box test in given in Figure 19. Dynamic bulk modulus (G) can be calculated using the inclination angle of the curve given in Figure 19 as drawing a line connecting the end points of the curve and given as;

$$G = \frac{\tau}{\gamma} \qquad (8)$$

τ is the repetitive shear stress, γ is the repetitive shear deformation. Dynamic shear modulus of the flow bands is calculated as 237 MPa using the equation (8).

The energy loss between the shape deformation occur under the repeated loads and the discontinuity surfaces is obtained as damping ratio. The energy loss controls whether the damping ratio is big or small for a material. The damping ratio is estimated using Figure 19 (D) as:

$$D = \frac{1}{4\pi} x \left(\frac{Histerisis\ circle\ area}{\substack{Area\ with\ in \\ the\ curve \\ triangular\ area}} \right)$$

$$D = \left(\frac{1}{4\pi}\right) x \left(\frac{AL}{AT}\right) \qquad (9)$$

AL is the total area in the histerisis, AT is the triangle area in the histerisis. Damping ratio (D) is calculated as 0.634 using the equation (9). Figure 19 shows the shear stress versus shear displacement curves (100 cycles) for flow bands. The andesites specimen is the same and equal to 9. Hence, the maximum shear stresses of andesites specimen were nearly the same, and reached around 2.10 MPa and -2.45 MPa, respectively, under applied normal load of 3.0 MPa. The absolute maximum shear stress of specimen for positive shear displacement phase is similar to that for negative shear displacement phase and reached around 3 MPa. The peak dynamic friction angle corresponding to specimen was computed based on the ratio between peak shear and normal stresses. The peak dynamic friction angle averaged after 100 cycles is given in Table 12.

Peak and residual shear strength of the flow bands were found as 6.00 MPa and 3.00 MPa under the σ_N =3 MPa normal stress and static conditions, respectively.

Table 12. Dynamic friction angles of the flow bands

Flow Bands	σ_N (MPa)	τ_P (MPa)	ϕ (°)
Positive phase	3	2.43	39
Negative phase	3	2.70	42
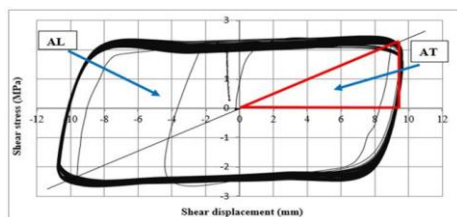
Figure 19. Shear stress versus shear displacement after shearing of 100 cycles of flow bands.

Shear strengths of the flow band structures are found as 2.70 MPa in 58. cycle and 2.43 MPa in 71. cycle under the dynamic conditions (Fig. 18). As a result, it was found that peak shear strength of dynamic conditions is 45 % lesser than the one in static conditions.

Peak internal friction angle of the flow bands and residual internal friction angle is calculated as 37° and 30° under the static conditions (σ_N =3 MPa normal stress), respectively (Fig. 15). Internal friction angle of the flow bands is calculated between the range of ϕ = 39° – 42° under the dynamic conditions.The variations in normal displacement with time for andesites specimen is shown in Fig. 20 respectively. The normal displacements behave like a harmonic function and continue to decrease with increasing time and number of cycles, respectively. The reason for increasing negative displacements (settlements) during the cyclic shearing is the ongoing degradation of the joint surface. However, the shear movement of one cycle can be subdivided into four different phases: forward advance, forward return, backward advance and backward return phase. The shear and normal displacements for andesite specimens are illustrated in Figure 21 for one cycle.
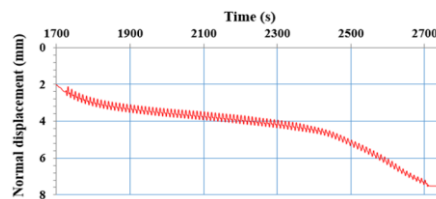
Figure 20. Normal displacement versus time of flow bands.
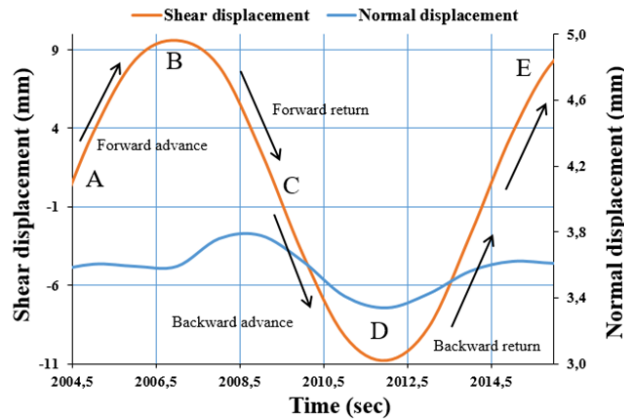
Figure 21. Shear and normal displacements versus time for five cycle of flow bands

The four phases can be characterized as follows:

Phase I (A to B): lower block is moved forward and due to slope direction dilation is negative (compression).

Phase II (B to C): lower block is moving into the opposite direction and due to slope direction dilation is positive (dilation). At point C the sample has reached again the original position.

Phase III (C to D): lower block is still moving into the opposite direction and dilation is still positive (dilation).

Phase IV (D to E): direction of lower block movement is returned and has the same direction as in phase I, due to slope direction dilation becomes negative (compression).

7. Results

Triaxial compression tests were conducted in static conditions and not only cohesion and internal friction angle values were obtained but also the values of Elasticity Modulus and Poisson's ratio (v_{40-60}) in interval of 0.4 $\sigma_1 \leq \sigma_u \leq 0.6 \sigma_1$ were calculated in these tests.

4kN/min axial force, 1 MPa/min cell pressure, 5 kN dynamic axial force applied for 300 seconds during the dynamic triaxial pressure tests, as a result these tests, ($\sigma_{1dyn\ min}$) and ($\sigma_{1dyn\ max}$) parameters were obtained.

The shear strength characteristics of flow bands in andesites were investigated considering various initial normal stresses, normal stiffnesses, shear velocities under CNL and dynamic boundary conditions. The direct shear tests were performed up to 20 MPa normal stress equivalent to more than 500 m in depth.

General results obtained from the static and dynamic shear box tests.

Shear box tests were conducted on 400 x 200 mm sized rectangle surfaces under the static and dynamic conditions. Time-deformation, time-stress, shear displacement-stress; shear displacement -normal displacement, shear displacement -shear stress, normal stress-shear stress relationships were obtained. In addition peak and residual shear strengths, base and residual friction angle values were obtained.

As shown in Figure 15 and Table 9, equations of the peak and residual shear strength envelopes are as follows;

$$\tau_P = 0.75.\sigma_n + 3.64 \; (R^2 = 0.98)$$

$$\tau_R = 0.58\sigma_n + 1.22 \; (R^2 = 0.99)$$

It is also seen in Figure 15 and Table 19 that the peak and the residual cohesion values and internal friction angles are 3,64 MPa, $\phi_P = 37°$ and 1.22 MPa, $\phi_R = 30°$ respectively.

Using the stress-strain relationship, histerisis curve, obtained from dynamic shear box test, dynamic bulk modulus (G) and damping ratio (D) were calculated. Using the histerisis curve obtained from the graph showing the relation between stress and deformation under the dynamic condition (dynamic shear box test), the values of dynamic Bulk modulus (G) and damping ratio (D) were calculated as 237 MPa and 0.634, respectively.

Reactions against the stress waves of andesitic flow bands and the effects of dynamic loadings on shear behavior of the flow band structures of andesites were investigated under the static and dynamic conditions in shear box tests. Static shear test was carried out under normal stress $\sigma_N = 3$ MPa. As a result, it was found to be peak shear stress $\tau_N = 6$ MPa and residuel shear stress $\tau_R = 3$ MPa for the flow bands in andesites. In the dynamic shear test the shear stress of 2.70 MPa at 58th cycle and 2.43 MPa at 71st cycle were found (Fig. 18). Thus, dynamic peak shear stress is 45% less than the static peak shear stress. Engineering properties of andesitic flow band were defined more realisticly using high pressure loadings and large scale shear box test apparatus. It will be possible to conduct realistic estimates related with earthquake occurences with the help of numerical software analysis using the earthquake sourced dynamic stability and instability data belonging to the andesitic flow bands.

References

[1] Ahola, M.P., Hsiung, S.M. and Kana, D.D., 1996. Experimental study on dynamic behavior of rock joints. *Developments in Geotechnical Engineering*. O. Stephansson, Jing, L., and Tsang, C.F. (Eds). Elsevier Science. 79: 467-494.

[2] Asadi, M.S. and Rasouli, V., 2012. Physical simulation of asperity degradation using laboratorial shear tests of artificial fractures. *Rock Engineering and Technology for Sustainable Underground Construction. ISRM International Symposium*. Stockholm**:** 1-14.

[3] ASTM 2002. Performing laboratory direct shear strength tests of rock specimens under constant normal force. *D-5607*: 1-12.

[4] Bakhtar, K. and Barton, N., 1984. Large scale static and dynamic friction experiments. *Proceedings of the 25th U.S. Symposium on Rock Mechanics*, The American Institute of Mining, Metallurgical and Petroleum Engineers**:** 457-466.

[5] Barbero, M., Barla, G. and Zaninetti, A., 1996. Dynamic shear strength of rock joints subjected to impulse loading. *Int. J. Rock Mech. Min. Sci.* 33 (2), 141-151.

[6] Barla G, Barla M, Camusso M, Martinotti, M.E., 2007. Setting up a new direct shear testing apparatus. *In: Proceedings of the 11th Congress of the International Society for Rock Mechanics, Lisbon, Portugal,* July 2007, Taylor & Francis, vol 1, pp 415–418.

[7] Barla G., Barla M., and Martinotti M.E., 2010. Development of a new direct shear testing apparatus.

Rock mechanics and Rock engineering, 43 (1), 117-122.

[8]   Barla, G., Barbero, M., Scavia, C., et al., 1990. Direct shear testing of single joints under dynamic loading. *Rock joints, Proceedings of International symposium*. N. Barton, and Stephansson, O., Eds. Loen, Balkema, Rotterdam**:** 447-454.

[9] Barton, N., 1976. The shear strength of rock and rock joints. *Int. J. Rock Mech. Min. Sci.* 13, 255-279.

[10] Belem, T., Mountaka, S. and Homand, F., 2004. Generalized directional peak shear stress criterion for dilatant rock joints. *57th Canadian Geotechnical Conference*. Quebec**:** 1-8.

[11] Belem, T., Souley, M. and Homand, F., 2007. Modeling surface roughness degradation of rock joint wall during monotonic and cyclic shearing. *Acta Geotechnica* 2 (4): 227-248.

[12] Boulon, M., 1995. A 3-D direct shear device for testing the mechanical behaviour and the hydraulic conductivity of rock joint. *Proc. of the MJFR-2 conf., Vienne, Autriche*, 407-413, Rossmanith ed., Balkema.

[13] Brady, B.H.G. and Brown, E.T., 2005. *Rock Mechanics for Underground Mining,* (Third edition), Kluwer Academic Publishers.

[14] Buzzi, O., Boulon, M., Herve, M., et al., 2008. Leaching of rock-concrete interfaces. *Rock Mechanics and Rock engineering* 41 (3): 445-466.

[15] DGGT (German Geotechnical Society) Empfehlung Nr. 1 des Arbeitskreises Versuchstechnik Fels (revised recommendation) 2004b. Einaxiale Druckversuche an zylindrischen Gesteinsprüfkörpern (Uniaxial compression tests on rock specimens). *Bautechnik* 81, 825 – 834.

[16] Divoux, P., Boulon, M. and Bourdarot, E., 1997. A mechanical constitutive model for rock and concrete joints under cyclic loading. *Proceedings of Damage and Failure of Interfaces*. H. P. Rossmanith, (Ed). Vienna, Austria**:** 443-450.

[17] Ferrero, A.M., Migliazza, M. and Tebaldi, G., 2010. Development of a new experimental apparatus for the study of the mechanical behaviour of a rock discontinuity under monotonic and cyclic loads. *Rock Mechanics and Rock Engineering* 43 (6), 685-695.

[18] Fox, D.J., Kana, D. D. and Hsiung, S. M., 1998. Influence of interface roughness on dynamic shear behavior in jointed Rock. *Int. J. Rock Mech. Min. Sci.* 35 (7): 923-940.

[19] Geertsema A.J., 2002. The shear strength of planar joints in mudstone. *Int. J. Rock Mech. Min. Sci.*, 39, 1045-1049.

[20] Gehle C., 2002. Bruch- und scherverhalten von gesteinstrennflächen mit dazwischenliegenden materialbrücken. In Published by Faculty of Civil Engineering, Ruhr-University Bochum.

[21] Gentier, S., Riss, J., Archambault, G., et al., 2000. Influence of fracture geometry on shear behavior. *Int. J. Rock Mech. Min. Sci.* 37, 161-174.

[22] Gomez, J.E., Filz, M.G., Ebeling, R.M., et al., 2008. Sand-to-Concrete interface response to Complex load paths in a large displacement shear box. *Geotechnical Testing Journal* 31 (4), 1-12.

[23] Grasselli, G. and Egger, P., 2003. Constitutive law for the shear strength of rock joints based on three-dimensional surface parameters. *Int. J. Rock Mech. Min. Sci* 40 (1), 25-40.

[24] Haberfield, C.M. and Seidel, J.P., 1999. Some recent advances in the modelling of soft rock joints in direct shear. *Geotechnical and Geological Engineering* 17, 177-195.

[25] Haque, A., 1999. Shear behaviour of soft rock joints under constant normal stiffness. *Published by Department of Civil, Mining and Environmental Engineering*, 1-293.

[26] Hobbs, B.E., Ord, A. and Marone, C., 1990. Dynamic behaviour of rock joints. *Rock joints, Proceedings of International symposium*. N. Barton, and Stephansson, O., (Eds). Loen, Balkema, Rotterdam, 435-445.

[27] Hoek, E., 2007. Practical Rock Engineering. *RocScience*: 1-237.

[28] Homand-Etienne, F., Lefevre, F., Belem, T., et al., 1999. Rock joints behavior under cyclic direct shear tests. *Proc. 37th U.S. Rock Mechanics Symp.* Colorado U.S.A, Balkema: 399-406.

[29] Huang, X., Haimson, B.C., Plesha, M.E., et al., 1993. An investigation of the mechanics of rock joints - part 1. laboratory investagation. *Int. J. Rock Mech. Min. Sci.* 30 (3), 257-269.

[30] Hutson, R.W. and Dowding, C.H., 1990. Joint asperity degradation during cyclic shear. *Int. J. Rock Mech. Min. Sci.* 27 (2), 109-119.

[31] ISRM 1974. Suggested methods for determining shear strength. Committee on standardisation of Laboratory and Field tests, pp 1–23.

[32] ISRM 2007. The complete ISRM suggested methods for rock characterization, testing and monitoring: 1974 – 2006. Compilation arranged by the ISRM Turkish National Group, Ankara, 2007.

[33] ISRM, 1981. Rock characterisation testing and monitoring ISRM suggested methods. Brown, E.T., (Editor), Pergamon Press.

[34] ISRM, 1983. Suggested methods for determining the strength of rock materials in triaxial compression. Revised version. Int. J. Rock Mech. Min. Sci. & Geomech. Abstr. 20, 285 – 290.

[35] Jafari, M.K., Hosseini, K.A., Pellet, F., et al., 2003. Evaluation of shear strength of rock joints subjected to cyclic loading. *Soil Dynamic and Earthquake Engineering* 23: 619-630.

[36] Jiang, Y., Li, B. and Tanabashi, Y., 2006. Estimating the relation between surface roughness and mechanical properties of rock joints. *Int. J. Rock Mech. Min. Sci.* 43, 837-846.

[37] Jiang, Y., Xiao, J., Tanabashi, Y., et al., 2004. Development of an automated servo-controlled direct shear apparatus applying a constant normal stiffness condition. *Int. J. Rock Mech. Min. Sci.* 41, 275-286.

[38] Jing, L., Stephansson, O. and Nordlund, E., 1993. Study of rock joints under cyclic loading conditions. *Rock Mechanics and Rock Engineering* 26 (3), 215-232.

[39] Kana, D.D., Fox, D.J. and Hsiung, S.M., 1996. Interlock/Friction model for dynamic shear response in natural jointed Rock. *Int. J. Rock Mech. Min. Sci.* 33 (4), 371-386.

[40] Kim D.Y., Chun, B.S. and Yang, J.S., 2006. Development of a direct shear apparatus with rock joints and its verification tests. *Geotechnical testing*, 29 (5).

[41] Kim, D.Y. and Lee, Y.N., 2007. New peak shear strength criteria for anisotropic rock joints using quantified joint roughness parameters. *11th Congress of the International Society for Rock mechanics*. Lisbon, 355-358.

[42] Koca, M.Y. & Kıncal, C., 2004. Abandoned stone quarries in and around the Izmir city centre and their geoenvironmental impacts. *Engineering Geology* 75, 49–67.

[43] Koca, M.Y., 1995. Slope stability assessment of the abandoned Andesite quarries in and around the Izmir city centre. PhD Dissertation. Dokuz Eylul University, Graduate School of Natural and Applied Science, Izmir, Turkey.

[44] Koca, M.Y., Ozden, G., Yavuz, A.B., Kıncal, C., Onargan, T. and Kucuk, K., 2006. Changes In Engineering Properties of Fire Exposed Marble Columns. *Int. Jour. of Rock Mech.& Min. Sci.*, Elsevier, Vol. 43, Issue 4.

[45] Kodikara, J.K. and Johnston, I.W., 1994. Shear behaviour of irregular triangular rock-concrete joints. *Int. J. Rock Mech. Min. Sci.* 31 (4), 313-322.

[46] Konietzky, H., Frühwirt, T., Luge, H., 2012b. A new large dynamic rockmechanical direct shear box device. *In: Rock Mechanics Rock Engineering*, 45 (3): 427-432.

[47] Konietzky, H., Frühwirt, T., Nguyen, V.M., 2012a. GS 1000: A new large rockmechanical shear box device for dynamic and HM-coupled testing under extreme strong froces. *In: Proc. EUROCK 2012*, 1-9.

[48] Lee, H.S., Park, Y.J., Cho, T.F., et al., 2001. Influence of asperity degradation on the mechanical behavior of rough rock joints under cyclic shear loading. *Int. J. Rock Mech. Min. Sci.* 38: 967-980.

[49] Luge, H., 2011. Entwicklung, Aufbau und Versuchssteuerung für ein neuartiges dynamisches hydro-mechanisches Felsschergerät für extrem hohe Kräfte. *Published by Geotechnical Institute*, TU Bergakademie Freiberg.

[50] Nguyen, V.M., 2013. Static and dynamic behaviour of joints in schistose rock: Lab testing and numerical simulation. Publ. Geotechnical Institute 2013-3 (ed. H. Konietzky), TU Bergakademie Freiberg, Germany.

[51] Ohnishi, Y. and Dharmaratne, P.G.R., 1990. Shear behaviour of physical models of rock joints under constant normal stiffness conditions. *Proceedings of the international conference on rock joints*, Balkema, Rotterdam**, 267-273.

[52] Qiu, X., Plesha, M.E., Huang, X., et al., 1993. An investigation of the mechancis of rock joints - Part II. Analytical investigation. *Int. J. Rock Mech. Min. Sci.* 30 (3), 271-287.

[53] Seidel, J.P and Haberfield, C.M., 2002. Laboratory testing of concrete-rock joints in constant normal stiffness direct shear. Geotechnical Testing, 25 (4).

[54] Wang, W.H., Li, X.B., Zhang, Y.P., et al., 2007. Closure behavior of rock joint under dynamic loading. *Jour. Cent. South Univ. Technol.*, 408-412.